Electron-capture delayed fission properties of the new isotope ^{238}Bk

S. A. Kreek,* H. L. Hall,* K. E. Gregorich, R. A. Henderson,† J. D. Leyba,‡ K. R. Czerwinski,§ B. Kadkhodayan,‖ M. P. Neu, C. D. Kacher, T. M. Hamilton, M. R. Lane, E. R. Sylwester, A. Türler,¶ D. M. Lee, M. J. Nurmia, and D. C. Hoffman

Chemistry Department, University of California, Berkeley and Nuclear Science Division, Lawrence Berkeley Laboratory, MS-70A/3307 Berkeley, California 94720

(Received 9 August 1993)

Electron-capture delayed fission ECDF was studied in the new isotope ^{238}Bk produced via the ^{241}Am(75-MeV $\alpha, 7n$)^{238}Bk reaction. The half-life of the fission activity was measured to be 144±5 seconds. The mass-yield distribution is predominantly asymmetric and the most probable preneutron emission total kinetic energy of fission is 179±7 MeV. The ECDF mode in ^{238}Bk was verified by an x-ray-fission coincidence experiment which indicated that the ^{238}Cm fission lifetime is between about 10^{-15} and 10^{-9} seconds. The isotope was assigned to ^{238}Bk through chemical separation and observation of the known 2.4-h ^{238}Cm daughter activity. No alpha branch was observed in the decay of ^{238}Bk. The production cross section for ^{238}Bk is 150±20 nb and the delayed fission probability is $(4.8\pm2)\times10^{-4}$.

PACS number(s): 23.40.−s, 21.10.Gv, 21.10.Tg, 27.90.+b

I. INTRODUCTION

Electron-capture delayed fission (ECDF) is an exotic nuclear decay process in which a nucleus undergoes electron-capture (EC) decay to excited states in its daughter, which then fission. The ECDF process is shown schematically in Fig. 1. This process is especially interesting because it allows study of the fission properties of nuclides whose fission branches are too small to allow detailed study of ground-state fission. Delayed fission (DF) is also believed to influence the production yields of heavy elements in multiple neutron-capture processes followed by β decay, such as in the stellar r process and nuclear weapons test [1–5]. A theoretical description of the DF process is given in Refs. [6–9].

Experimentally, the ECDF probability, P_{ECDF}, is defined as the ratio of the number of electron-capture decays resulting in a fission, N_{ECDF}, to the total number of electron-capture decays, N_{EC}:

$$P_{\mathrm{ECDF}} = \frac{N_{\mathrm{ECDF}}}{N_{\mathrm{EC}}} .$$

The neutron-deficient berkelium region was chosen for several reasons. First, ECDF branches have been reported, previously, in neutron-deficient neptunium [10], americium [11–13], einsteinium [10], and berkelium [10] isotopes. Second, the electron-capture Q value (Q_{EC}) for the neutron-deficient isotopes approaches the height of the fission barriers of about 5–5.5 MeV in these regions [14] and therefore, ECDF is expected to be an important decay mode. Isotopes with a Q_{EC} value larger than about 4 MeV should begin to have measurable ECDF branches. Nuclides with sufficient Q_{EC}'s are found in the region of very neutron-deficient odd-proton, odd-neutron nuclei, which have enhanced EC Q values associated with decay to their more stable even-even daughters. Neutron-deficient odd-proton–odd-neutron neptunium isotopes, such as ^{228}Np, which has a calculated [15]

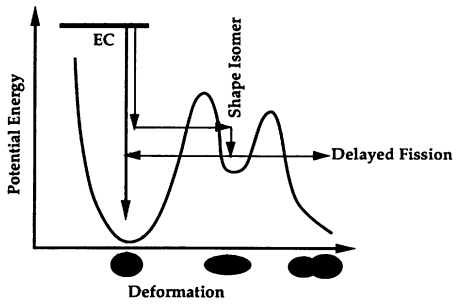

FIG. 1. Two-dimensional schematic diagram of potential energy vs deformation for the delayed fission process. Electron-capture decay with large Q values can populate excited states which can be above the fission barrier or within the first potential energy well or within the second potential energy well.

*Present address: Nuclear Chemistry Division, L-231 Lawrence Livermore National Laboratory, Livermore, CA 94550.

†Present address: EG&G Rocky Flats, Inc., Rocky Flats Plant, P.O. Box 464, Golden, CO 80402.

‡Present address: Clemsen Technical Center, Inc., 100 Technology Dr., Anderson, SC 29625.

§Present address: Institut für Radiochemie, Technische Universität München, Walther-Meissner-Str. 3, D-8046 Garching, Germany.

‖Present address: Glenn T. Seaborg Institute for Transactinium Science, L-396 Lawrence Livermore National Laboratory, Livermore, CA 94550.

¶Present address: Paul Scherrer Institute, Würenlingen und Villigen, Ch-5232 Villigen, Switzerland.

 ©1994 The American Physical Society

Q_{EC} of 4.65 MeV, should have significant branches for ECDF decay.

Several experiments must be performed in order to identify the ECDF process. First, a short-lived, anomalous fission activity must be detected in a region where the spontaneous fission (SF) half-lives are expected to be long. The half-life of the anomalous fission activity as well as the fission properties such as the mass-yield distribution and total kinetic energy, TKE, can then be measured. Second, a time correlation between the electron-capture x rays and the fission activity must be established. Such a time correlation experiment gives positive identification of the ECDF process, and was first performed by Hall *et al.* [11] in 1989 in the study of ^{234}Am. The x-ray energies from EC yield the Z of the EC parent. The Z can also be confirmed radiochemically. Third, the mass must be assigned by detection of known decay progeny in chemically separated samples.

II. EXPERIMENT

A. Targets and irradiation

The ^{241}Am targets were prepared by electrodeposition [16–19] on 2.3-mg/cm^2 Be foil. Beryllium was chosen as the target support because it was necessary to have target backings that would withstand large beam intensities, would not seriously degrade the beam energy, and would be mechanically strong.

A sample containing 150-mg ^{241}Am was obtained in the form of Am_2O_3. It was dissolved in about 3-mL concentrated HCl and dried. The $AmCl_3$ was redissolved in 1 mL of 0.1-M HCl and the Am was extracted into 1 mL of 0.5-M bis-2-ethylhexyl-o-phosphoric acid (HDEHP) in heptane [20–22]. The Am^{3+} is extracted into the HDEHP while impurities such as Na^+ remain in the aqueous phase. The HDEHP phase was removed and the Am^{3+} was back extracted into 1 mL of concentrated HCl. The Np^{5+} daughter remained in the HDEHP phase. The solution of $AmCl_3$ was dried and converted to $Am(NO_3)_3$ by dissolving the $AmCl_3$ in 1.0-mL concentrated HNO_3 and drying. This process was repeated several times. The conversion to the nitrate form was required because the Be foil is subject to chemical attack by chloride. This would reduce the effectiveness of the plating procedure and make the resulting target unsafe for bombardment in the accelerator. An aliquot of the final Am^{3+}/HNO_3 solution was dried and the $Am(NO_3)_3$ was dissolved in 1.0 mL of isopropanol (IPA). An aliquot of the IPA solution was dried on Pt foil and assayed by alpha-pulse-height analysis.

An electroplating cell was prepared and an appropriate amount of the $Am(NO_3)_3$/IPA solution was added so that a target about 80 μg/cm^2 would be produced. The Am was electroplated from the IPA at 0.8 mA and 300 V for 30 min on the 2.3-mg/cm^2 Be backings. The electroplated sample was then baked in an oven at 400 °C for 30 min. The diameter of the deposit was 0.95 cm, resulting in an area of 0.71 cm^2 for each target. The targets were glued to Al supports for use in the Light Ion Multiple Target System (LIM) [23]. The amount of ^{241}Am present in each target was determined by gamma-ray analysis with a Ge detector.

Nine mounted ^{241}Am targets were placed in the LIM [23] with approximately 2-cm distance between them. A 4.6-mg/cm^2 Be foil served as the volume limiting foil, and another similar Be foil served as the vacuum window for the target system.

A 75-MeV $^4He^{2+}$ beam of 3–4 pμA was provided by the Lawrence Berkeley Laboratory 88-Inch cyclotron. The beam energy was about 73 MeV on the first target. The reaction products were swept from the target system with a He/KCl aerosol jet which transported the activities through a 1.4-mm i.d. polyvinyl chloride capillary tube to either our rotating-wheel system for fission and half-life measurements or to a nearby chemistry hood for collection and subsequent x-ray–fission coincidence measurements or chemical separation and alpha-pulse-height measurements.

B. Rotating-wheel measurements

For measurement of the fission properties, the activity laden aerosols were transported to our "Merry-Go-around" (MG) rotating-wheel system [24] and deposited on 79 polypropylene foils (40 ± 10 μg/cm^2 thick) positioned around the periphery of a 51-cm-diam wheel. The sources were stepped at preset intervals of 2 min and positioned successively between six pairs of passivated ion-implanted silicon (PIPS) detectors which were positioned directly above and below the sample. This arrangement gave an efficiency of approximately 60% for detection of coincident fission fragments. Energy and time information for each detected fission fragment was recorded in list mode with our "Real-Time Data Acquisition and Graphics System" (RAGS) [25]. The system was calibrated using ^{252}Cf sources on similar polypropylene foils. Subsequent sorting and histogramming were performed on the data to extract fission-fragment energy spectra, coincidence data, and half-life information.

C. X-ray–fission correlation measurement

The activity laden KCl aerosols were collected on Ta foil which was taped to a 1-mm-thick fiberglass stick. The diameter of the deposit was approximately 2 mm. The activity was placed before a light-tight transmission-mounted 300-mm^2 silicon surface barrier (SSB) detector operated in air which was sandwiched between two germanium x-ray detectors as shown in Fig. 2.

Because an average of approximately 8–10 prompt γ rays are emitted [26,27] from the fission fragments, a high overall γ-detection efficiency would reject many of the true x-ray events due to summing effects. However, too low a detection efficiency would reduce the observed correlation rate. This problem was resolved as described in Refs. [11,28].

The overall uranium $K\alpha$ x-ray–SF coincidence detec-

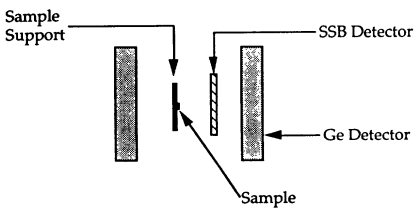

FIG. 2. X-ray–fission detector configuration. The solid-state detector (SSB) is sandwiched between two Ge detectors.

tion efficiency was determined to be 11.8% by measuring the 5.81-MeV alpha particles from a ^{249}Cf source in coincidence with the $K\alpha$ x-rays of the Cm daughter. The Cm $K\alpha$ x-ray intensities from the ^{249}Cf alpha decay are given in Ref. [29]. The ratio of the total number of coincident Cm $K\alpha$ x rays to the total number of ^{249}Cf alpha events yields the $K\alpha$ x-ray–SF efficiency. Appropriate amplifier gains for fission fragments were determined with a ^{252}Cf source evaporated on a 11.5-mg/cm^2 Ni foil. Prompt γ-ray summing effects were estimated by measuring the γ rays in coincidence with fission fragments from a ^{252}Cf source. The ratio of the number of γ-ray–fission coincidences to the total number of fissions yields the fraction lost by summing. It is assumed that any differences in the γ-ray multiplicities between the SF of ^{252}Cf and the ECDF of ^{238}Bk are negligible.

The signal from the SSB detector provided a common start for two time-to-amplitude converters (TAC's). The stop signals were provided by the first and second germanium γ-ray detectors. The time window on the TAC's was ±500 nsec. The timing resolution of the germanium detectors was approximately 9-nsec full width at half maximum (FWHM), and the energy resolution of each detector was less than 1.5-keV FWHM in the Cm K x-ray region. Upon detection of a fission fragment in the SSB detector, the amplitudes of the pulses in the SSB detector, the γ-ray detectors, and the TAC's were recorded with RAGS.

D. Chemical separations

Two methods of chemical separation were employed in the study of ECDF in ^{238}Bk. The elemental and mass assignment utilized the well-known 3+/4+ oxidation state couple for Bk and an HDEHP extraction of the 4+ state [20–22]. The Bk was oxidized with a saturated solution of $KBrO_3$ in concentrated HNO_3 and the Bk^{4+} was extracted into 0.5M HDEHP in heptane. The organic phase was removed, and the Bk was reduced and back extracted into 3M HCl containing 1% H_2O_2. The isolated Bk fraction was dried on Ta foil and analyzed for alpha and fission activities.

The x-ray–fission correlation procedure required an initial separation of all activities from the monovalent ^{22}Na produced by interactions of the ^{4}He beam with the aluminum target holders due to a slight target system misalignment. The Bk and other activities were removed from the Na by extraction into 0.5-M thenoyltrifluoroacetone (TTA) in benzene. This complexing agent is known to extract 3+ and higher oxidation state species quite readily from aqueous solutions between pH 4 and 5 [30]. The produced activities were dissolved in a buffered solution of acetic acid and sodium acetate maintained at pH 5 and then extracted into the TTA. The TTA phase, containing the Bk, was removed and evaporated on Ta foil for analysis.

III. RESULTS AND DISCUSSION

A. Half-life and fission properties

Samples resulting from 2.0-min collections of the KCl aerosol on polypropylene foils were stepped consecutively between the six pairs of PIPS detectors in the MG system. After one complete revolution of the MG wheel (79 collections), the wheel was replaced with a clean one to prevent further buildup of KCl and any long-lived fission activities.

During the course of three experiments, 739 pairs of coincident fission fragments were detected. The half-life was determined to be 144±5 sec by a least-squares analysis of these 739 events. The decay curve is shown in Fig. 3. Each point in the fit was normalized to represent the same number of samples. This is necessary since before the data acquisition is stopped, detector station one measures 79 samples, station two measures 78 samples, station three measures 77 samples, and so on.

Appropriate detector gains for fission fragments were determined from ^{252}Cf sources evaporated on Ni foils. Coincident fission fragment calibrations were obtained using ^{252}Cf sources on 40 μg/cm^2 polypropylene foils. Approximately 15 000 pairs of coincident fission frag-

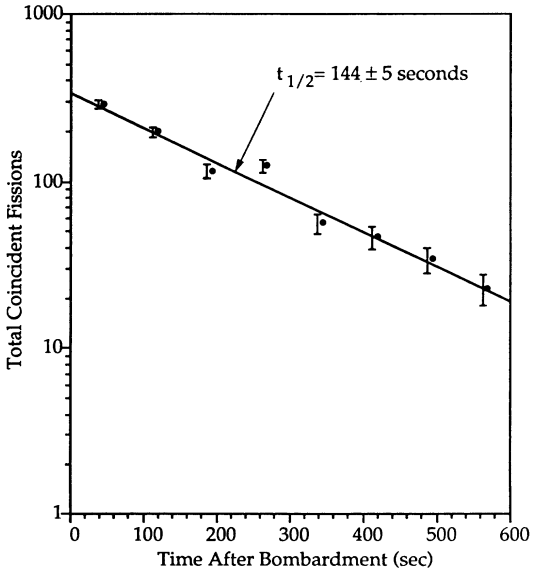

FIG. 3. Least-squares fit to coincident fissions from ECDF of ^{238}Bk as measured on MG-RAGS. Data correspond to 388 individual experiments (collections). The half-life was determined to be 144 ± 5 sec.

ments from the ^{252}Cf standards were detected per detector station.

A total of 382 pairs of coincident fission fragments were detected in two of the experiments and the kinetic energies of the fragments were determined. The off-line fission fragment energy calibrations were obtained by the method of Schmitt, Kiker, and Williams [31] using the constants of Weissenberger *et al.* [32]. The average neutron emission function, $\bar{\nu}(A)$, was taken as similar to that of ^{252}Cf, normalized to an average neutron emission of $\bar{\nu}_t = 2.0$ (estimated from systematics in Ref. [26]). The mass-yield distribution of the ECDF of ^{238}Bk and the ^{252}Cf calibration standard is shown in Fig. 4. The mass-yield distribution for the ECDF of ^{238}Bk is predominantly asymmetric. The TKE distribution for the ECDF of ^{238}Bk, without correction for energy degradation in the KCl, is shown in Fig. 5. The most probable preneutron TKE for the ECDF of ^{238}Bk was determined from this distribution to be 174 ± 5 MeV. The TKE distribution shown in Fig. 5 shows a low-energy tail. This may be partially a result of energy straggling due to sample thickness. Effects of fission-fragment energy degradation from the polypropylene foil were the same for the ^{238}Bk data as for the ^{252}Cf calibration sources which were on similar polypropylene foils. The average fission fragment energy

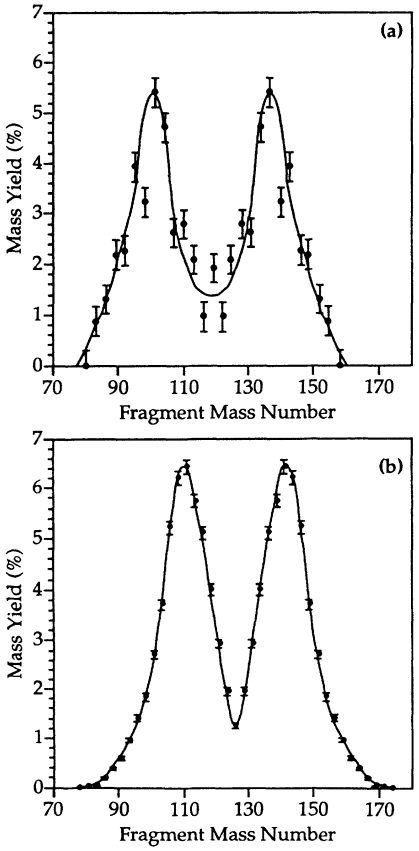

FIG. 4. (a) Preneutron emission mass-yield distribution for the ECDF of ^{238}Bk. The data were averaged over 3 mass numbers. (b) Preneutron emission mass-yield distribution of ^{252}Cf.

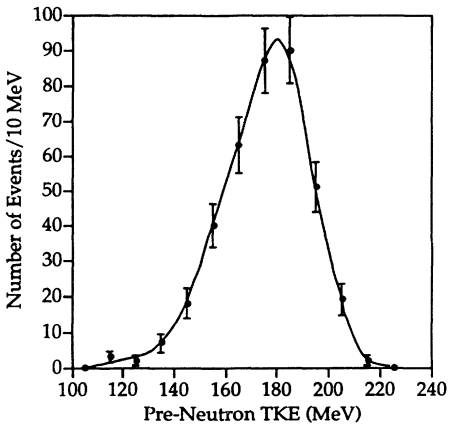

FIG. 5. Preneutron emission TKE distribution (not corrected for energy degradation in the KCl) for the ECDF of ^{238}Bk. The data are in groupings of 10 MeV.

degradation from the KCl in the ^{238}Bk collections [33] ($0.5\ \mu g\,cm^{-2}\,sec^{-1}$) was estimated to be about 3 MeV for the heavy fragment and 2 MeV for the light fragment. The energy loss was estimated from Fig. 2c of Appendix 17 in Ref. [29], assuming a 0.7-MeV/nucleon heavy fragment, and a 1-MeV/nucleon light fragment. The most probable preneutron TKE for the ECDF of ^{238}Bk was estimated to be 179 ± 7 MeV, after correction for the estimated 5 MeV degradation in the KCl. This TKE value is similar to that predicted by the systematics of Viola [34]. Figure 6 is a plot of the average or most proba-

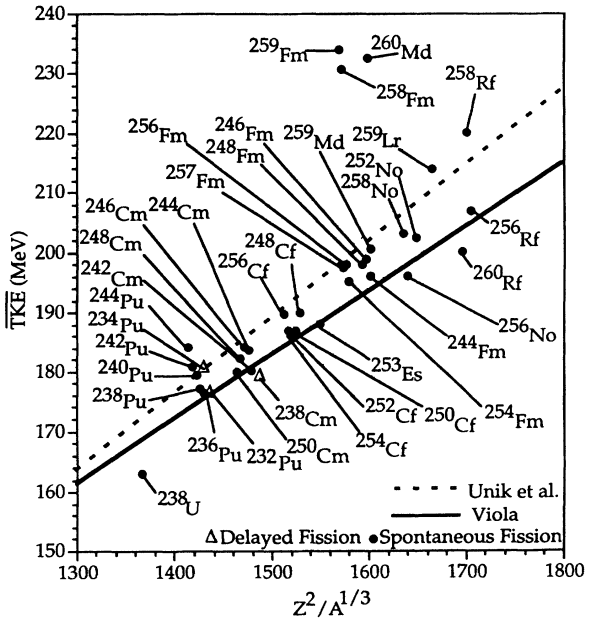

FIG. 6. Average or most probable TKE vs $Z^2/A^{1/3}$. The solid line is the linear fit of Viola [34]. The dashed line is from Unik *et al.* [37]. All of the $\overline{TKE}$ values have been corrected to be consistent with the calibration parameters of Weissenberger *et al.* [32]. The open triangles depict values measured for delayed fission. The closed circles depict values measured for spontaneous fission.

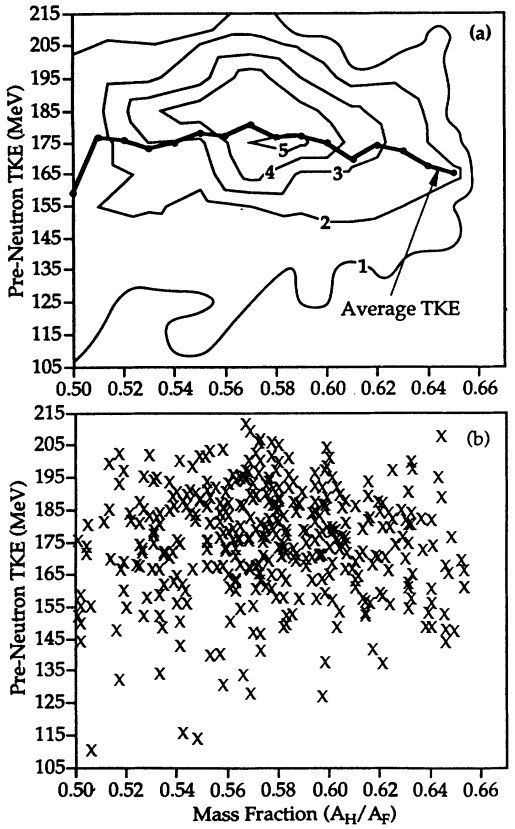

FIG. 7. (a) Contour diagram of data for ECDF of ^{238}Bk as a function of preneutron-emission TKE and MF. The contours indicate equal numbers of events based on data groupings of 10 MeV × 0.02 units of mass fraction. Contours 1–5 indicate 5, 10, 15, 20, and 25 events, respectively. The average TKE at each mass fraction (not corrected for energy degradation in the KCl) is indicated. A total of 382 events are included. (b) Individual events from ECDF of ^{238}Bk plotted as a function of TKE and MF. A total of 382 events is illustrated.

ble TKE vs $Z^2/A^{1/3}$ for all known spontaneous fission and delayed fission isotopes. The most probable preneutron TKE for ^{232}Pu and ^{234}Pu, first reported by Hall *et al.* [6,7], were not corrected for fission-fragment energy degradation in the KCl deposit. This necessitates an increase of about 2 and 7 MeV to the previously reported most probable TKE values for the ECDF of ^{232}Am, and ^{234}Am, respectively. These new values are included in Fig. 6 and are similar to those predicted by the systematics of Viola (Ref. [34]).

The TKE vs mass fraction (MF) contour diagram for the ECDF of ^{238}Bk is given in Fig. 7(a). The actual TKE vs MF data are given in Fig. 7(b). No correction to the energies were made for absorption in the KCl. (MF is defined as MF= A_H/A_F, where A_H is the mass number of the heavy fragment; A_F is the mass number of the fissioning nucleus.)

According to the static scission point model of Wilkins *et al.* [35], the asymmetric mode in the ECDF of ^{238}Bk should have one spherical ($\beta_s = 0.1$, $Z = 52$, $N = 80$) and one deformed fragment ($\beta_d = 0.4$, $Z = 44$, $N = 62$). The symmetric mode should have either two near spherical fragments ($\beta_s = 0.2$, $Z = 48$, $N = 71$) or two highly deformed fragments ($\beta_d = 0.7$, $Z = 48$, $N = 71$), depending on the deformation chosen for $N = 71$. the neutron contour diagram in Ref. [35] shows two possible deformations for $N = 71$. High and low TKE components at symmetric mass splits are possible because of the significantly different deformations possible for fragments with $N = 71$. The deformation parameters, β_d (deformed fragment) and β_s (spherical fragment), are estimated from the proton and neutron contour diagrams given in Ref. [35].

TABLE I. Efficiency and summing information for the germanium and the solid-state detectors used in the study of ECDF in ^{238}Bk. Because the samples were dried on Ta foils, a correction was applied for absorption by the Ta foil of 100-keV photons. The calculated number of expected correlations for the detector behind the Ta foil was corrected.

Experiment 1	Gamma 1	Gamma 2	SSB
Fission efficiency			80%
X-ray efficiency	8.6%	9.6%	
γ-ray summing	30%	40%	
Fissions detected			208
Expected Number of corrections	12	12	
Correction for absorption of Ta		6	
Total expected x-ray–fission correlations	18 ± 4		

Although the mass-yield distribution for the ECDF of ^{238}Bk given in Fig. 4 shows a higher yield at symmetry than the ^{252}Cf calibration standard, the poor statistics and energy degradation in the KCl deposits made it impossible to determine whether there is an enhanced yield of symmetric mass splits. Similarly, it is not clear whether two groupings of events at high and low TKE's at mass fraction 0.50 corresponding to the two different fragment configurations in the symmetric fission discussed previously (see Fig. 7) are present.

B. X-ray–fission correlation results

Approximately 800 samples were prepared with the TTA chemistry described earlier and 208 fission fragments were observed in the x-ray–fission coincidence system shown in Fig. 2. From previous work [6,7,10] and the determined detection efficiencies and summing rates, it was expected that 18 ± 4 x rays in the curium K x-ray energy region should be detected. Table I gives the efficiency and summing information for the germanium detectors and the efficiency of the solid-state detector (SSB) for the experiment. The expected number of x-ray–fission correlations in each detector is calculated from

$$\text{no. correlations} = \sum_{\gamma \text{ detectors}}^{\text{all}} (\text{no. fissions})(\text{x-ray efficiency})(1 - \gamma \text{ summing}) \ .$$

This equation assumes that only K electron capture contributes, no gamma transitions are K converted, and the K fluorescence yield is 100%.

It should be noted that a correction of approximately a factor of 2 was applied to the number of expected x-ray-fission correlations in the Gamma 2 detector to account for the x-ray events lost due to absorption in the Ta foil. The correction to the number of expected events in the Ge detector, which was positioned on the opposite side of the Ta foil, was obtained from the tables of photon ranges in matter in Ref. [29].

The Cm $K\alpha 2$ and $K\alpha 1$ peaks appear at 104.6 and 109.3-keV and the $K\beta 1+3$ and $K\beta 2$ peaks at 123 and 127 keV, respectively [29]. The observed x-ray–fission correlation data are shown in Fig. 8. We observed 17±4 x rays in the Cm K x-ray energy region. No more than 1 or 2 of these are likely due to prompt γ rays which leaves approximately 15±4 compared to the expected 18 x rays.

The observed number of prompt γ rays relative to the ^{238}Bk EC x rays indicates that the prompt γ-ray multiplicity from ^{238}Bk ECDF is similar to that from the SF of ^{252}Cf. The pileup rate was less than about 2% because the γ-ray singles rate was less than 10^4 sec^{-1}. This was monitored occasionally during the experiment with an oscilloscope.

It is assumed that the fissioning states populated by the EC decay are high in excitation energy. For ^{238}Bk, electron capture from the K shell cannot populate states larger in excitation energy than about 4.5 MeV (the Q_{EC} minus the K-shell binding energy). Because of the small EC transition energy, it is possible that L capture plays a significant role in the ECDF process. Using the same technique involved in the calculation of the expected number of K x-ray–fission correlations, the total number of L_β and L_γ x-ray–fission correlations was expected to be 4 ± 1. This number includes the significantly lower fluorescence yield of L x rays ($\approx$ 18–49 %) compared to K x rays (98%) [36]. The possibility that the ECDF proceeds via L capture was ruled out because only 1 of the expected 4 Cm L x rays was detected in the x-ray–fission correlation experiment (see Fig. 8). This is consistent with the estimate that about 1 L x-ray correlation would result from conversion after K capture based on data from the table of x-ray intensities given in Ref. [36]. It is likely that the absence of L x-ray–fission correlations indicates that fission occurs primarily from levels populated by EC transition energies larger than the K-shell edge.

The observation of 15 ± 4 K x rays is consistent with the expected 18 ± 4 K x rays and indicates that the K vacancies filled before fission of ^{238}Cm occurred. This may indicate that ECDF in ^{238}Bk proceeds via a fission shape isomer in the EC daughter and that the shape change associated with tunneling through the first barrier is faster than 10^{-17}–10^{-15} sec. If the shape change to the second potential well were slower than 10^{-15} sec, gamma decay to levels deep within the ^{238}Cm first potential well would dominate and the P_{DF} would be zero. The limit of the fission lifetime is 10^{-15}–10^{-9} sec. If the fission occurred faster than 10^{-15} sec, fewer than expected K x-ray–fission coincidences would have been detected. If the fission occurred more slowly than 10^{-9} sec, a delay would have been observed in the TAC spectrum.

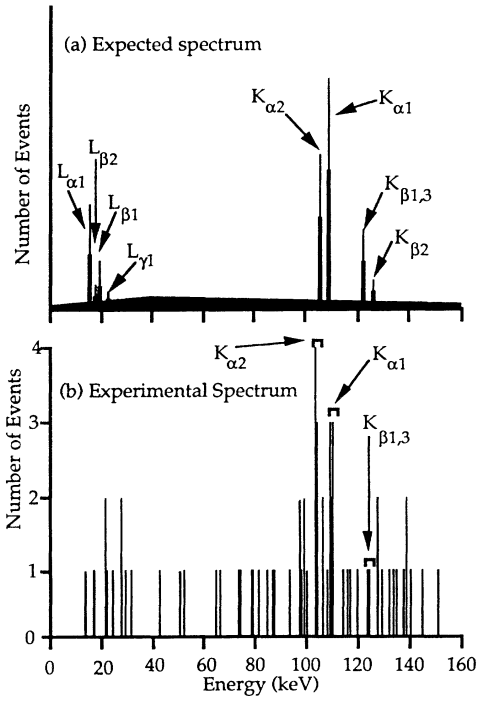

FIG. 8. X-ray–fission correlation data from ECDF of ^{238}Bk. (a) shows the expected x-ray spectrum with $K\alpha 1$ and $K\alpha 2$ peaks at 109.3 and 104.6 keV, and $K\beta 1+3$, and $K\beta 2$ peaks at 123 and 127 keV, respectively [29], together with an approximate expected energy distribution for the prompt γ-ray coincidences from the deexcitation of fission fragments. Possible contributions form L capture are also shown. (b) gives the experimental spectrum showing the 17 events detected in the Cm K x-ray region between 104 and 123 keV.

C. Decay modes of ^{238}Bk

No evidence for an alpha branch in the decay of ^{238}Bk with a 144 ± 5 second half-life was observed. No activity could be attributed to the 8.8-MeV alpha of ^{214}At, genetically related by alpha decay to ^{238}Bk, in chemically separated Bk samples. The electron-capture decay was confirmed by observation of the 6.52-MeV alpha decay of the 2.4-h ^{238}Cm daughter. The alpha-decay chains for ^{238}Bk and ^{238}Cm are shown in Fig. 9. The ^{238}Cm decay was consistent with a 2.4-h half-life. Because no alpha branch was observed in the decay of ^{238}Bk, it was assumed that the isotope decays primarily by EC. It is difficult to conclude that ^{238}Bk has no alpha branch, because the daughter ^{234}Am decays only 0.4% by alpha emission. If the ^{238}Bk also has only a small alpha branch, detection of the daughters further down the decay chain is very difficult. The ^{238}Bk was produced by the reaction ^{241}Am(75-MeV $\alpha, 7n$)^{238}Bk. The production cross section was calculated to be 150 ± 20 nb assuming an 80% He-jet yield and 80% chemical yield.

A delayed fission probability of $(4.8\pm2)\times10^{-4}$ was

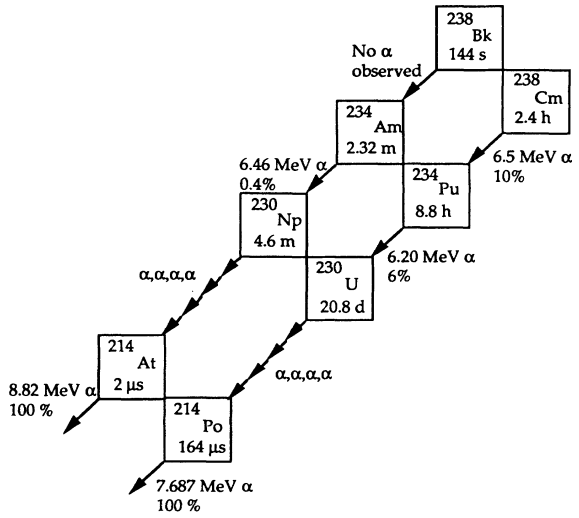

FIG. 9. Alpha-decay chains for ^{238}Bk and ^{238}Cm.

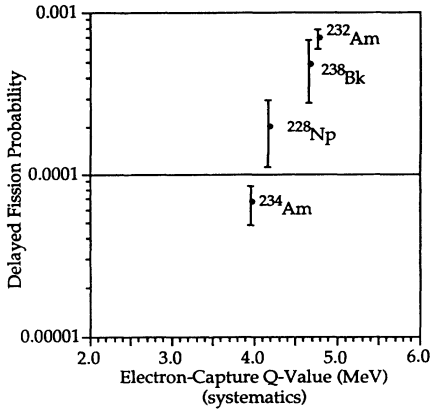

FIG. 10. The delayed fission probability vs the electron-capture Q value (Q_{EC}). The Q_{EC} values were taken from Ref. [14]. The delayed fission probabilities for ^{232}Am, ^{234}Am, and ^{228}Np were taken from Refs. [6,7,28], respectively.

calculated from the assumed electron-capture branch of 100%, the production cross section, and the fission rate of 5 ± 1 fission fragment pairs/h/eμA observed in the rotating-wheel experiments. This value is consistent with the values of 6.9×10^{-4} and 6.6×10^{-5}, respectively, determined for ^{232}Am and ^{234}Am by Hall *et al.* [6,7], and 2.0×10^{-4} for ^{228}Np determined by Kreek *et al.* [28], given the differences in the estimated EC Q values. Figure 10 is a plot of the delayed fission probabilities reported for ^{228}Np, ^{232}Am, ^{234}Am, and ^{238}Bk. The EC Q values were taken from the systematics of Möller *et al.* [14]. The apparent linear relationship between ECDF probability and Q_{EC} may indicate that the fission barrier heights remains fairly constant in the region between ^{228}Np and ^{238}Bk.

IV. CONCLUSIONS

ECDF was studied in the new isotope ^{238}Bk produced via the ^{241}Am$(\alpha, 7n)^{238}$Bk reaction. The fission properties and half-life were measured with a rotating-wheel system. The half-life of this new isotope was determined to be 144 ± 5 sec from measurements of the fission activity. An asymmetric mass-yield distribution was observed for the fissioning species with a most probable preneutron emission TKE of 179 ± 7 MeV. The observed fissions were assigned to ECDF in Bk by observation of fissions in coincidence with the x rays of Cm resulting from K capture in Bk. The mass and Z were assigned to ^{238}Bk by observation of the ^{238}Cm alpha chain and fissions in chemically separated Bk samples. The electron-capture branch in ^{238}Bk is assumed to be 100%. The production cross section for ^{238}Bk produced via the ^{241}Am$(\alpha, 7n)^{238}$Bk reaction is 150 ± 20 nb. The delayed fission probability is $(4.8 \pm 2) \times 10^{-4}$.

ACKNOWLEDGMENTS

The authors wish to thank the staff and crew of the Lawrence Berkeley Laboratory 88-Inch Cyclotron for their assistance and the Lawrence Livermore National Laboratory for providing the ^{241}Am target material. This work was supported in part by the U.S. Department of Energy through the Division of Nuclear Physics of the Office of High Energy and Nuclear Physics under Contract No. DE-AC03-76SF00098.

[1] E. M. Burbidge, G. R. Burbidge, W. A. Fowler, and F. Hoyle, Rev. Mod. Phys. **29**, 547 (1957).
[2] C.-O. Wene and S. A. E. Johansson, Phys. Scr. A **10**, 156 (1974).
[3] C.-O. Wene, Astron. Astrophys. **44**, 233 (1975).
[4] H. V. Klapdor, T. Oda, J. Metzinger, W. Hillebrandt, and F. K. Thielman, Z. Phys. A **299**, 213 (1981).
[5] B. S. Meyer, W. M. Howard, G. J. Matthews, K. Takahashi, P. Möller, and G. Leander, Phys. Rev. C **39**, 1876 (1989).
[6] H. L. Hall, K. E. Gregorich, R. A. Henderson, C. M. Gannett, R. B. Chadwick, J. D. Leyba, K. R. Czerwinski, B. Kadkhodayan, S. A. Kreek, D. M. Lee, M. J. Nurmia, D. C. Hoffman, C. E. A. Palmer, and P. A. Baisden, Phys. Rev. C **41**, 618 (1990).
[7] H. L. Hall, K. E. Gregorich, R. A. Henderson, C. M. Gannett, R. B. Chadwick, J. D. Leyba, K. R. Czerwinski, B. Kadkhodayan, S. A. Kreek, N. J. Hannink, D. M. Lee, M. J. Nurmia, D. C. Hoffman, C. E. A. Palmer, and P. A. Baisden, Phys. Rev. C **42**, 1480 (1990).
[8] E. E. Berlovich and Yu. P. Novikov, Dokl. Akad. Nauk SSSR **185**, 1025 (1969) [Sov. Phys. Dokl. **14**, 349 (1969)].
[9] H. L. Hall and D. C. Hoffman, Annu. Rev. Nucl. Part. Sci. **42**, 147 (1992).
[10] D. Habs, H. Klewe-Nebenius, V. Metag, B. Neumann, and H. J. Specht, Z. Phys. A **285**, 53 (1978).

[11] H. L. Hall, K. E. Gregorich, R. A. Henderson, C. M. Gannett, R. B. Chadwick, J. D. Leyba, K. R. Czerwinski, B. Kadkhodayan, S. A. Kreek, D. M. Lee, M. J. Nurmia, and D. C. Hoffman, Phys. Rev. Lett. **63**, 2548 (1989).
[12] Yuan-Fang Liu, Cheng Luo, K. J. Moody, D. Lee, G. T. Seaborg, and H. R. Von Gunten, J. Rad. Chem. **76**, 119 (1983).
[13] Yu. P. Gangrskii, M. B. Miller, L. V. Mikhailov, and I. F. Kharisov, Yad. Fiz. **31**, 306 (1980) [Sov. J. Nucl. Phys. **31**, 162 (1980)].
[14] H. C. Britt, E. Cheifetz, D. C. Hoffmann, and J. B. Wilhelmy, Phys. Rev. C **21**, 761 (1980).
[15] P. Möller, W. Meyers, W. Swiatecki, and J. Treiner, At. Data Nucl. Data Tables **39**, 225 (1988).
[16] V. B. Dedov and V. N. Kosyakov, *Proceedings of the International Conference on Peaceful Uses of Atomic Energy* (United Nations, New York, 1956), Vol. 7, pp. 369–373.
[17] J. E. Evans *et al.*, Nucl. Instrum. Methods **102**, 389 (1972).
[18] D. C. Aumann and G. Müllen, Nucl. Instrum. Methods A **115**, 75 (1974).
[19] G. Müllen and D. C. Aumann, Nucl. Instrum. Methods **128**, 425 (1975).
[20] J. B. Knauer and B. Weaver, Oak Ridge National Laboratory Report ORNL-TM-2428, 1968.
[21] G. H. Higgins, *The Radiochemistry of the Transcurium Elements*, Subcommittee on Radiochemistry, National Academy of Sciences, National Research Council (U.S. Atomic Energy Commission, Washington, D.C., 1960).
[22] D. F. Peppard, S. W. Moline, and G. W. Mason, J. Inorg. Nucl. Chem. **4**, 344 (1957).
[23] H. L. Hall, M. J. Nurmia, and D. C. Hoffman, Nucl. Instrum. Methods A **276**, 649 (1989).
[24] D. C. Hoffman, D. Lee, A. Ghiorso, M. Nurmia, and K. Aleklett, Phys. Rev. C **22**, 1581 (1980).
[25] R. G. Leres, Lawrence Berkeley Laboratory Report LBL-24808, 1987.
[26] D. C. Hoffman and M. M. Hoffman, Annu. Rev. Nucl. Sci. **24**, 151 (1974).
[27] D. C. Hoffman and L. P. Somerville, in *Charged Particle Emission from Nuclei*, edited by D. N. Poenaru and M. Ivascu (CRC, Boca Raton, 1989), Vol. III, p. 1.
[28] S. A. Kreek, Ph.D. thesis, Lawrence Berkeley Laboratory Report No. LBL-33766, 1993.
[29] *Table of Isotopes*, 7th ed., edited by C. M. Lederer and V. S. Shirley (Wiley, New York, 1978).
[30] A. M. Poskanzer and B. M. Foreman, Jr., J. Inorg. Nucl. Chem. **16**, 323 (1961).
[31] H. W. Schmitt, W. E. Kiker, and C. W. Williams, Phys. Rev. **137**, B837 (1965).
[32] E. Weissenberger, P. Geltenbort, A. Oed, F. Gönnenwein, and H. Faust, Nucl. Instrum. Methods A **248**, 506 (1986).
[33] K. E. Gregorich (private communication).
[34] V. E. Viola, Nucl. Data A **1**, 391 (1966).
[35] B. Wilkins, E. P. Steinberg, and R. R. Chasman, Phys. Rev. C **14**, 1832 (1976); B. Wilkins (private communication).
[36] E. Browne and R. B. Firestone, *Table of Radioactive Isotopes* (Wiley, New York, 1986).
[37] J. P. Unik *et al.*, *Proceeding of the Third International IAEA Symposium on the Physics and Chemistry of Fission*, Rochester, 1973 (IAEA, Vienna, 1974), Vol. II, p. 33.

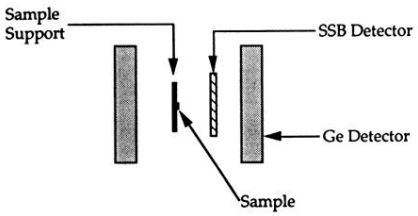

FIG. 2. X-ray–fission detector configuration. The solid-state detector (SSB) is sandwiched between two Ge detectors.